VIROLOGY 197, 53–63 (1993)

Analysis of *cis*-Acting Sequences Essential for Coronavirus Defective Interfering RNA Replication

YOUNG-NAM KIM, YONG SEOK JEONG, AND SHINJI MAKINO[1]

Department of Microbiology, The University of Texas at Austin, Austin, Texas 78712-1095

Received May 11, 1993; accepted July 14, 1993

Mouse hepatitis virus (MHV) defective interfering (DI) RNA was used to determine the *cis*-acting sequences required for MHV RNA replication. A 2.2-kb-long cDNA clone of the MHV DI RNA DIssE was used to test the effect of deletions throughout the DI RNA on replication in DI RNA-transfected, MHV-infected cells. Data from a series of deletion mutants demonstrated that about 470 nucleotides at the 5′ terminus, 460 nucleotides at the 3′ terminus, and about 135 nucleotides in an internal position approximately 0.9 kb from the 5′ end of DI RNA were necessary for DI RNA replication. These data suggested that *cis*-acting sequences which were necessary for MHV RNA replication required not only terminal sequences but also an internal sequence present at about 3.2 kb from the 5′ end of the genome.

INTRODUCTION

An infectious virus genome contains *cis*-acting replication elements recognizable by virus-specific proteins and probably by host cell factors. This recognition of RNA by protein is essential for RNA virus genome replication. One way to identify the *cis*-acting replication signals on an RNA virus genomic sequence is to analyze its defective interfering (DI) RNA. DI RNA replication occurs, in general, only in the presence of helper virus. Therefore, DI RNA must contain sequences required for replication. Using cloned Sindbis virus DI cDNAs, Levis *et al.* have successfully identified the sequences essential for replication and packaging of that virus (1986). The *cis*-acting RNA replication signals of several plant viruses belonging to the alphavirus superfamily (Ahlquist *et al.*, 1985) have been identified by deletion analysis of the smallest segmented genomic RNA, which is not necessary for viral RNA replication (French and Ahlquist, 1987; Gilmer *et al.*, 1992; Jupin *et al.*, 1990; Pacha *et al.*, 1990). Another approach identifying *cis*-acting RNA replication signals on the negative-stranded RNA virus genome of influenza virus has been developed (Luytjes *et al.*, 1989). However, identification of the *cis*-acting RNA replication signals of many other RNA viruses, including coronavirus, has not been reported.

Mouse hepatitis virus (MHV), a coronavirus, is an enveloped virus containing a single-stranded, positive-sense RNA genome of approximately 31 kb (Lai and Stohlman, 1978; Lee *et al.*, 1991; Pachuk *et al.*, 1989). In MHV-infected cells, seven or eight species of virus-specific mRNAs with a 3′-coterminal nested-set structure (Lai *et al.*, 1981; Leibowitz *et al.*, 1981) are synthesized; these are numbered 1 to 7, in decreasing order of size (Lai *et al.*, 1981; Leibowitz *et al.*, 1981). None of the mRNAs are packaged into MHV virions, except for mRNA 1, which is efficiently packaged due to the presence of a packaging signal (Fosmire *et al.*, 1992). The 5′ end of MHV genomic RNA contains a 72- to 77-nucleotide-long leader sequence (Lai *et al.*, 1983, 1984; Spaan *et al.*, 1983). This is the only copy of the leader sequence in the genome. However, this sequence is found at the 5′ end of each MHV message; in each mRNA, the leader sequence becomes fused with the mRNA body sequence at its 5′ intergenic-consensus sequence (Joo and Makino, 1992; Lai *et al.*, 1983, 1984; Makino *et al.*, 1988b; Spaan *et al.*, 1983). The activity which synthesizes all MHV-specific RNA species is detected continuously at least during the first 6 hr of infection (Jeong and Makino, 1992).

When the JHM strain of MHV (MHV-JHM) is serially passaged in tissue culture at a high multiplicity of infection, a variety of different sized DI RNAs are detected (Makino *et al.*, 1984a, 1985). The complete sequences of two MHV-JHM-derived DI RNAs, DIssE and DIssF, are known (Makino *et al.*, 1988a, 1990). The 2.2-kb-long DIssE, which is the smallest DI RNA detected so far, consists of three noncontiguous genomic regions. The first region (domain I) represents 0.86 kb from the 5′ end of the genomic RNA. The second region (domain II), 0.75 kb, corresponds to the region 3.1 to 3.9 kb from the 5′ end of genomic RNA. The third domain (domain III) represents 0.6 kb from the 3′ end of the parental MHV-JHM genome. The 3.4-kb-long DIssF RNA, which is packaged efficiently into the MHV

[1] To whom reprint requests should be addressed.

0042-6822/93 $5.00

virion due to the presence of a packaging signal (Fosmire *et al.*, 1992; Makino *et al.*, 1990), consists of five noncontiguous genomic regions (Makino *et al.*, 1990). Interestingly, domains I and II of DIssE are present in DIssF, and the junction between these two domains is identical in both DIs (Makino *et al.*, 1990). The 3′-most domain of DIssF, domain V, represents 447 nucleotides from the 3′ end of the MHV-JHM genome and is shorter by 155 nucleotides at the 5′ end than the corresponding region of DIssE (Makino *et al.*, 1990). Two other DIssF regions not found in DIssE are derived from gene 1 (Makino *et al.*, 1990). Sequence analysis of a 5.5-kb MHV-A59-derived DI RNA, DI-a, revealed the presence of three noncontiguous regions from the MHV-A59 genome: the 5′-terminal 3.9 kb, a 0.8-kb fragment from the 3′ end of the gene 1, and the 3′-terminal 805 nucleotides (van der Most *et al.*, 1991). Therefore, all the MHV DI RNAs so far sequenced contain the sequences found in DIssE domains I and II and domain V of DIssF. RNase T1 oligonucleotide fingerprint analysis of MHV-JHM-derived DI RNAs revealed that all the oligonucleotides present in DIssE are present in all other DI RNAs (Makino *et al.*, 1985). This conservation of sequence indicates that, quite possibly, all MHV DI RNAs share most of the sequence of DIssE and that these sequences are essential for MHV replication in general. It is not known how much of the DIssE sequence is necessary for MHV DI RNA replication.

A system was established in which complete cDNA clones of both DIssE and DIssF RNAs were placed downstream of the T7 RNA polymerase promoter to generate DI RNAs capable of extremely efficient replication in the presence of a helper virus (Makino and Lai, 1989). This system using cloned MHV DI cDNA has been shown to be useful for analysis of coronavirus RNA replication (Kim *et al.*, 1993; Makino and Lai, 1989), RNA transcription (Jeong and Makino, 1992; Joo and Makino, 1992, Makino and Joo, 1993, Makino *et al.*, 1991), RNA recombination (de Groot *et al.*, 1992; Kim *et al.*, 1993; van der Most *et al.*, 1992) and RNA packaging (Fosmire *et al.*, 1992; Makino *et al.*, 1990; van der Most *et al.*, 1991). In the present study, it is used to identify MHV *cis*-acting replication signals. A series of DIssE-derived deletion mutants were constructed and their replication was examined in the presence of helper virus. The data demonstrated that not only the terminal sequences of the DI RNA but also 0.13 kb from the domain II 5′ end were necessary for efficient MHV DI RNA replication.

MATERIALS AND METHODS

Viruses and cells

The plaque-cloned MHV-A59 (Lai *et al.*, 1981) was used as a helper virus. Mouse DBT cells (Hirano *et al.*, 1974) were used for growth of viruses.

DNA construction

The names of all oligonucleotides and the locations of their DI RNA binding sites are shown in Fig. 1.

Deletion of internal sequences. An *Eco*RV site was put into a DIssE cDNA by a procedure using recombinant polymerase chain reaction (PCR) (Higuchi, 1990). DIssE-specific cDNA clone DE5-w4 (Makino and Lai, 1989) was incubated with two oligonucleotides, oligonucleotide 1453 (5′-CAAACTAGTTAAGAGCG-3′), which hybridizes to nucleotides 1489 to 1505 from the 5′ end of DE5-w4, and oligonucleotide 2063 (5′-CTTTCTGATATCGATCGTTTGTCC-3′), which contains an *Eco*RV site and hybridizes to nucleotides 1737 to 1760 from the 5′ end of DE5-w4, at 93° for 30 sec, 37° for 40 sec, and 72° for 100 sec in PCR buffer (0.05 *M* KCl, 0.01 *M* Tris–hydrochloride [pH 8.0], 0.0025 *M* $MgCl_2$, 0.01% gelatin, 0.17 m*M* each deoxynucleoside triphosphate, and 5 U of Taq polymerase [Promega]) for 25 cycles. The same PCR condition was used for all DNA constructions. The PCR product was obtained by incubating DE5-w4 with oligonucleotide 130 (5′-TTCCAATTGGCCATGATCAA-3′) (Makino *et al.*, 1991), which hybridizes to nucleotides 2182–2202 from the 5′ end of DE5-w4, and with oligonucleotide 963 (5′-CAAACGATCGATATCAGAAAGATGAAGTAGA-3′), which contains an *Eco*RV site and hybridizes at 1736 to 1759 nucleotides from the 5′ end of DE5-w4. Two PCR products of the expected size were mixed and the second round of PCR was performed using oligonucleotide 1453 and oligonucleotide 130 as the primers. The 0.71-kb *Spe*I–*Msc*I PCR product was cloned into the *Spe*I–*Msc*I large fragment of MC 136-1 (Makino *et al.*, 1991), yielding MRC.

A series of mutants deleted internally upstream from the MRC *Eco*RV site were constructed. Mutants MR1, MR2, MR3, MR4, and MR6 were missing the 1.27-kb-long *Stu*I–*Eco*RV fragment, the 1.05-kb *Eag*I–*Eco*RV fragment, the 0.66-kb *Sph*I–*Eco*RV fragment, the 0.26-kb *Spe*I–*Eco*RV fragment, and the 0.13-kb *Sca*I–*Eco*RV fragment, respectively. Mutant MR5 was constructed by inserting the 0.32-kb MRC *Sna*BI–*Fsp*I fragment into the 2.88-kb MRC *Sna*BI–*Eco*RV fragment.

MR9 was constructed by self-ligating the 4.21-kb *Eag*I–*Sph*I MRC fragment. MR9B was made from MRC by incubating it with oligonucleotide 1567 (5′-CCTCTGCTGCGCAAGAA-3′) which hybridizes the MRC 5′ end at nucleotides 333 to 348, and with oligonucleotide 1940 (5′-ATACAACATCTGTTGCATTAAAGTCATACACA-3′), which hybridizes to nucleotides 850 to 881 also from the 5′ end. The PCR products were blunt-ended, phosphorylated, and digested with *Eag*I and the 0.18-kb product was isolated and inserted into the large *Sph*I–*Eag*I MRC fragment. MR9C was made similarly using oligonucleotide 2167 (5′-TATGACTCGGCCGCAACAGATGTTGT-3′), which contains an *Eag*I site and

hybridizes to nucleotides 853 to 879, and oligonucleotide 1942 (5′-GTAGAGTACTATCAAATCTCTTTAGACAACGCCAGTT-3′) which hybridizes to nucleotides 1599 to 1630 for the PCR and, from this PCR reaction, the 0.79-kb *Eag*I–*Spe*I fragment was isolated for insertion into the large MRC *Eag*I–*Spe*I fragment. MR9D was made by inserting the 0.49-kb *Fsp*I–*Spe*I MRC fragment into the large *Eag*I–*Spe*I MRC fragment. MR9E was constructed by inserting the 0.30-kb *Eag*I–*Fsp*I MRC fragment into the large *Eag*I–*Sph*I MRC fragment. MR8 was constructed by self-ligation of the 4.38-kb MRC *Stu*I–*Eag*I fragment. Two PCR products were obtained by incubating MRC with oligonucleotide 96 (5′-CACTTCCTGCGTGTCCAT-3′), which hybridizes to 85 to 102 from the 5′ end of MRC, and oligonucleotide 1128 (5′-TCACGGATTATGGCGGA-3′) which hybridizes at 429 to 445 from the 5′ end of MRC, and by incubating MRC with oligonucleotide 96 and oligonucleotide 167 (5′-CTTCTGGGGATCCTCGTC-3′), which hybridizes at 457 to 474; both PCR products were blunt ended, phosphorylated and digested with *Nco*I. The 0.19-kb PCR product obtained using oligonucleotides 96 and 1128 was inserted into the *Eag*I–*Nco*I MRC large fragment, yielding MR10B. The 0.21-kb PCR fragment obtained using oligonucleotides 96 and 167 was inserted into the *Eag*I–*Nco*I MRC large fragment, yielding MR10C. For the MR7, the 0.32-kb MRC *Sna*BI–*Fsp*I fragment was inserted into the MRC 4.15-kb *Sna*BI–*Stu*I fragment. MR8N was the result of inserting the 0.47-kb *Sna*BI–*Stu*I fragment from clone NE1 (Kim *et al.,* 1993) into the 3.9-kb *Sna*BI–*Eag*I MRC fragment. A PCR product was obtained by incubating MRC with oligonucleotides 2167 and 1942. This PCR product was digested with *Eag*I and *Fsp*I, and the resultant 0.13-kb fragment was inserted into the MRC *Stu*I–*Eco*RV large fragment, yielding MRD.

Deletion of 5′-terminus. MR13 resulted from insertion of the 0.65-kb *Dra*I–*Eag*I MRC fragment into the large *Sna*BI–*Eag*I MRC fragment. Clones MR14 and MR15 were made after construction of intermediate clone, JMP 102. To make JMP 102, the DIssF-specific cDNA clone DF2-1 was constructed using the same procedure as DF1-2 (Makino *et al.,* 1990), except that DNA fragment derived from DE-1A (Makino and Lai, 1989) was used instead of DE5-w4 (Makino and Lai, 1989). A PCR product was obtained by incubating DF2-1 with oligonucleotide 52 (5′-AAGCTTAATACGACTCACTATAGTATAAGAGTGATTGGCGTCCGTAC-3′) (Makino and Lai, 1989), and oligonucleotide 1249 (5′-CACGCAGGGATATCCGTTTA-3′), which contains the *Eco*RV site and hybridizes to nucleotides 74 to 93 from the 5′ end of DF2-1. Another PCR product was obtained by incubating DF2-1 with oligonucleotide 167 and oligonucleotide 1248 (5′-TAAACGGATATCCCTGCGTG-3′), which also has the *Eco*RV site and hybridizes to nucleotides 74 to 93 from the 5′ end of DF2-1. The two PCR products resulting from those incubations were mixed and incubated with oligonucleotides 52 and 167. The 0.44-kb *Sna*BI–*Bam*HI PCR product was inserted into the corresponding region of DF2-1, yielding JMP102. A plasmid was constructed by removing the 21-nucleotide-long *Dra*I–*Eco*RV fragment of JMP102. The 1.1-kb *Hin*dIII–*Sph*I fragment of this plasmid DNA was put into the large *Hin*dIII–*Sph*I MRC fragment, resulting in MR14. For the construction of MR15, a PCR product was obtained by incubating the JMP102 with oligonucleotides 52 and 1249. This PCR product was digested with *Eco*RV, phosphorylated and blunt-ended, and inserted into the large *Afl*III MRC fragment. For the construction of MR16, the 0.33-kb MRC *Nco*I fragment and the 0.18-kb *Afl*III–*Hin*dIII fragment were ligated and digested with *Hin*dIII and *Stu*I, and the resultant 0.49-kb *Hin*dIII–*Stu*I fragment was inserted into the large *Hin*dIII–*Stu*I MRC fragment. For MR17, a PCR product was obtained by incubating MRC with oligonucleotides 1567 and 1940; the 0.36-kb *Fsp*I–*Eag*I PCR product was inserted into the large *Nco*I–*Eag*I MRC fragment. MRE construction required two separate PCR reactions: one used MRC and oligonucleotides 52 and 1249, and the other used MRC with oligonucleotide 1568 (5′-TCTGCATATGCAACATC-3′), which hybridizes at 872–882 from the 5′ end of MRC, and oligonucleotide 1248. Recombinant PCR was performed by incubating those two PCR products with oligonucleotides 52 and 1568. The 0.68-kb *Sna*BI–*Eag*I PCR product was inserted into the large *Sna*BI–*Eag*I MRC fragment, yielding MRE.

Deletion of 3′-terminus. For MR11, the 0.43-kb *Alu*I–*Xba*I MRC fragment was ligated with the large *Sph*I–*Xba*I MRC fragment. To make MR19, MRC was incubated with oligonucleotide 1 (5′-CCATAGATATCATAATGGCA-3′), which hybridizes at positions 198 to 217 from the 5′ end of MRC, and oligonucleotide 2165 (5′-ATTTCGGGTTACCGAGCTTTTGGG-3′), which has a *Bst*EII site and hybridizes 1785 to 1809 nucleotides from the 5′ end of MRC. The 1.65-kb *Alu*I–*Bst*EII PCR fragment was cloned into the large MRC *Bst*EII fragment, yielding MR19. MR20 construction used a plasmid deleted at the 0.46-kb *Sna*BI–*Stu*I fragment and the 0.18-kb *Bst*EII–*Ban*I fragment of MRC. The 1.13-kb-long *Sph*I–*Xba*I fragment of this plasmid was inserted into the *Sph*I–*Xba*I MRC large fragment. For the construction of MR21, a PCR product was obtained by incubation of MRC with oligonucleotides 1453 and 130 and the 0.18-kb *Spe*I–*Ban*I fragment was inserted into the *Spe*I–*Msc*I MRC large fragment. For each mutant the entire region obtained by insertion of the PCR product was sequenced.

RNA transcription and transfection

Plasmid DNAs were linearized by *Xba*I digestion and transcribed with T7 RNA polymerase as previously de-

scribed (Makino and Lai, 1989). Lipofection was used for RNA transfection as previously described (Makino *et al.*, 1991).

Preparation of virus-specific intracellular RNA and agarose gel electrophoresis

Virus-specific RNAs in virus-infected cells were labeled with ^{32}Pi as previously described (Makino *et al.*, 1984b). For the study of negative-strand RNA, RNA was extracted according to the procedure of Sawicki and Sawicki (1990) with a slight modification as previously described (Kim *et al.*, 1993). Virus-specific RNA was separated by electrophoresis on 1% agarose gels after denaturation with 1 *M* glyoxal (MaMaster and Carmichael, 1977).

RT-PCR

For the amplification of negative-stranded MHV RNA species, MHV-specific cDNA was first synthesized from intracellular RNA as previously described (Makino *et al.*, 1988a), using as a primer oligonucleotide 96, which binds to negative-stranded DI RNA at nucleotides 81 to 98 from the 3′ end. After cDNA synthesis, reverse transcriptase (RT) was inactivated by heating the sample to 100° for 10 min. MHV-specific cDNA was then incubated with oligonucleotide 1568, which binds to positive-sense DI RNA at nucleotides 872 to 888 from the 5′ end, in PCR buffer at 93° for 30 sec, 55° for 30 sec, and 72° for 100 sec for 25 cycles. For the amplification of positive-stranded DI RNA, MHV-specific cDNA was first synthesized from intracellular RNA, using as a primer oligonucleotide 1568. After cDNA synthesis, MHV-specific cDNA was then incubated with oligonucleotide 52 in PCR buffer under the same conditions used for the amplification of negative-stranded RNA species.

Direct sequencing of the PCR product

The PCR products were separated by agarose gel electrophoresis and recovered from the gel slices by using GeneClean II (Bio 101, La Jolla, CA). Direct PCR sequencing was performed as previously described (Joo and Makino, 1992; Winship, 1989).

RESULTS

Effects of internal sequence deletions on MHV DI RNA replication

To determine whether the entire DIssE sequence was necessary for MHV DI RNA replication, a series of DIssE-derived DI cDNAs, each with a different length internal deletion, was constructed and the replication of those mutants was examined in DI RNA-transfected, MHV-infected cells. A parental clone, MRC, was constructed from DIssE (Fig. 1). The structures of MRC and MHV-JHM-derived DIssE were very similar, except that the 5′ end 463 nucleotides of MRC were MHV-A59-derived, and MRC contained several mutated nucleotides within the sequences present from positions 1743 to 1751. These nucleotide substitutions created an *Eco*RV site (Fig. 1B). The 3′-most domain of DIssF, domain V, contains 447 nucleotides from the 3′ end of the MHV genome and is shorter by 155 nucleotides at the 5′ end than the corresponding region of DIssE (Makino *et al.*, 1990). The sequence downstream of nucleotide 1767 in MRC included all of domain V of DIssF (Fig. 1B). Replication of this series of deletion mutants, each with the same sequence downstream of the *Eco*RV site, but with gradational deletions upstream, was examined (Figs. 2 and 3). Equal amounts of *in vitro-synthesized mutant DI RNAs and MRC DI RNA* were transfected by lipofection into DBT cell monolayers infected with MHV-A59 helper virus 1 hr prior to transfection (Makino *et al.*, 1991). Virus-specific RNAs were labeled with ^{32}Pi in the presence of actinomycin D (Makino *et al.*, 1984b) and analyzed by agarose gel electrophoresis. Efficient replication of MRC, MR3, MR4 and MR6 was observed, whereas MR5, MR1, and MR2 replication was not detected (Fig. 3). All replicating DI RNAs had the predicted sizes, indicating that the deleted sequences were maintained in the transfected cells. This data demonstrated that MRC nucleotides 1095 to 1751 were not necessary for efficient DI RNA replication, and that all or part(s) of the sequence(s) from nucleotides 703 to 1095 was necessary for efficient DI RNA replication.

Nucleotides 703 to 1095 were further analyzed to determine the smallest sequence necessary for replication. Mutants successively deleted within nucleotides 703 to 1095 were constructed, and their replication was examined in DI RNA-transfected, MHV-infected cells (Figs. 2 and 3). Replication of MR9, deleted at nucleotides 706 to 1093, was not observed. This observation was consistent with the data obtained above. MR9C contained all of the domain II sequence, minus nucleotides 706 to 865; that deletion corresponds to the most 3′-region of domain I. As shown in Fig. 3, MR9C replicated efficiently, demonstrating that the most 3′ 0.16 kb of domain I was not necessary for efficient DI RNA replication. Replication was not observed for MR9B and MR9D, with deletions of nucleotides 881 to 1093 and 706 to 999, respectively. The mutant MR9E, deleted at nucleotides 999 to 1093, did replicate efficiently (Figs. 2 and 3). MR9C and MR9E RNAs had their expected sizes in DI RNA-transfected cells, and the replication efficiency of both was lower than that of MRC. This series of experiments showed that of the nucleotides present from position 706 to 1093, those from 706 to 865 and 999 to 1093 were not nec-

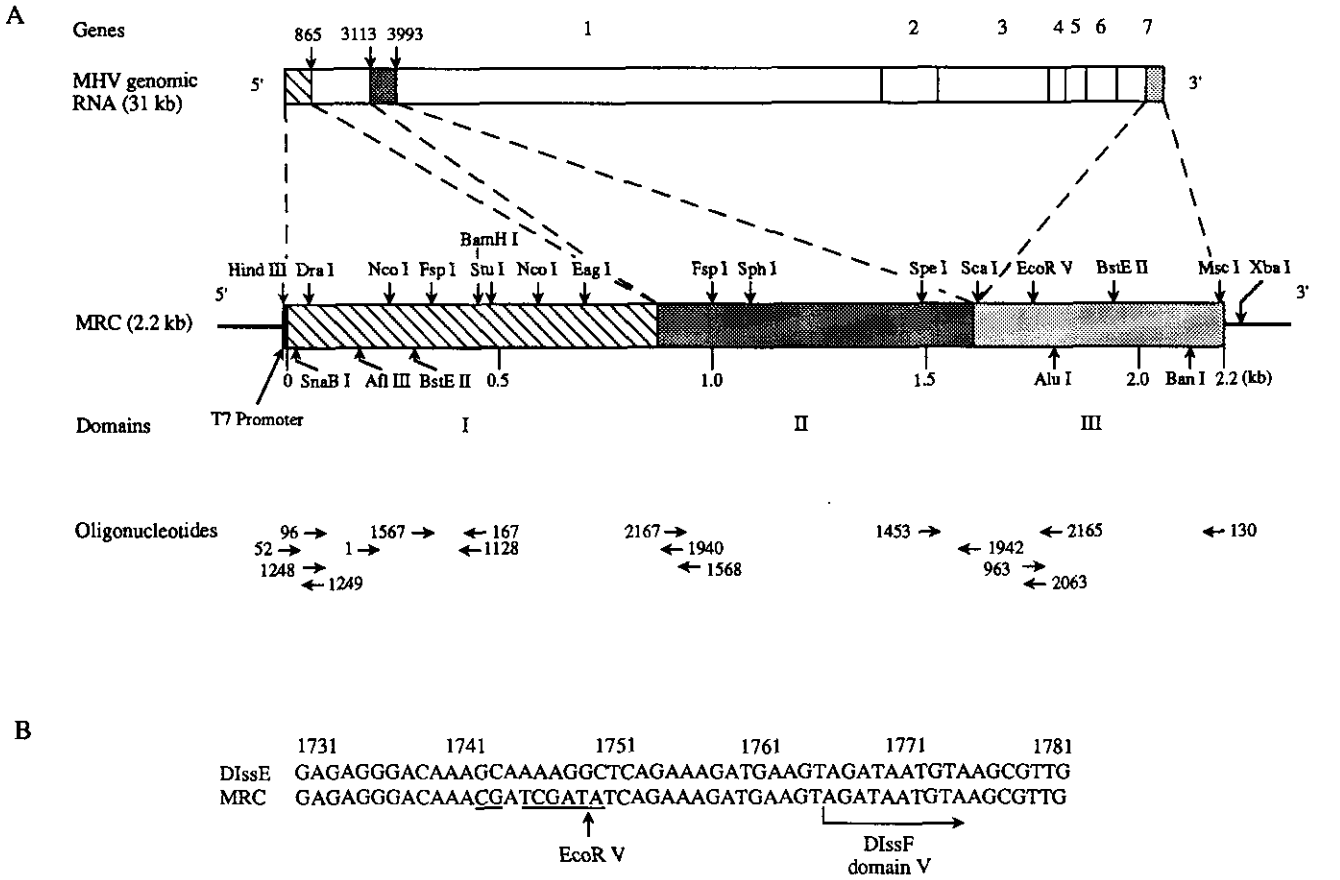

FIG. 1. Schematic diagram of the structure of DIssE-derived mutant MRC. (A) The structure of DIssE-derived MRC is compared with that of the standard MHV-genomic RNA. Genes 1 through 7 represent the seven genes of MHV. Three domains of DIssE (domains I through III) are indicated beneath the diagram of MRC; the exact location of I and II on MHV genomic RNA is shown as nucleotides numbered from the 5' end of MHV-JHM. Restriction enzyme sites used in the construction of the deletion mutants and the *Eco*RV site created in MRC are shown. The names of all oligonucleotides are shown beneath the diagram of MRC, and the locations of their MRC binding sites are indicated with arrows. Thin lines in the diagram of MRC represent vector sequences. (B) Sequence difference between DIssE and MRC. The MRC sequences which are different from DIssE are underlined. The sequence downstream of the nucleotide position 1767 in MRC is identical to DIssF domain V.

essary for efficient DI RNA replication, and that the 5' region of domain II, the 134-nucleotide long sequence from position 865 to 999, was required for efficient replication.

To further identify the MHV *cis*-acting RNA replication signals, several graded deletions within the sequence present from nucleotides 342 to 708 were created and the replication of these mutants was examined in DI RNA-transfected, MHV-infected cells (Figs. 2 and 3). DI RNAs deleted at positions 482 to 706 (MR8) and 474 to 708 (MR10C) replicated efficiently in DI RNA-transfected cells (Fig. 3). Both replicating DI RNAs had their expected sizes in DI RNA-transfected cells and replicated slightly less efficiently than MRC, demonstrating that nucleotides 474 to 708 were not necessary for efficient DI RNA replication. Replication of DI RNAs deleted at nucleotides 445 to 708 (MR10B) and 342 to 482 (MR7) was not observed, suggesting that all or part(s) of the sequence present between nucleotides 342 and 474 was necessary for efficient DI RNA replication.

The data above showed that MR6, MR8, MR9E, and MR10C, with an incomplete DIssE-specific ORF, replicated efficiently. This observation was consistent with the observation that the DIssE-specific large ORF need not be intact for efficient DIssE RNA replication in DI RNA-transfected, MHV-infected cells (Kim *et al.*, 1993). To confirm that the failure of DI RNA replication in MR2, MR9B, MR9D, and MR10B, all of which contained an interrupted ORF, was not due to the absence of the large DIssE-specific ORF, MR8N, which had a one-nucleotide deletion at nucleotide 376, was constructed; the ORF of MR8N terminated at nucleotide 383 (Fig. 2). As shown in Fig. 3, MR8N replicated efficiently. In some experiments, it was found that MR8N replicated slightly less efficiently than MR8 in other experiments the replication levels were the same (data not shown). RNA from MR8N-transfected cells was sequenced to verify the maintenance of the mutation after transfection. This was done in a way that avoided detection of the amplified input DI RNAs, which are known to be present in a small quantity as late as 6 hr post-trans-

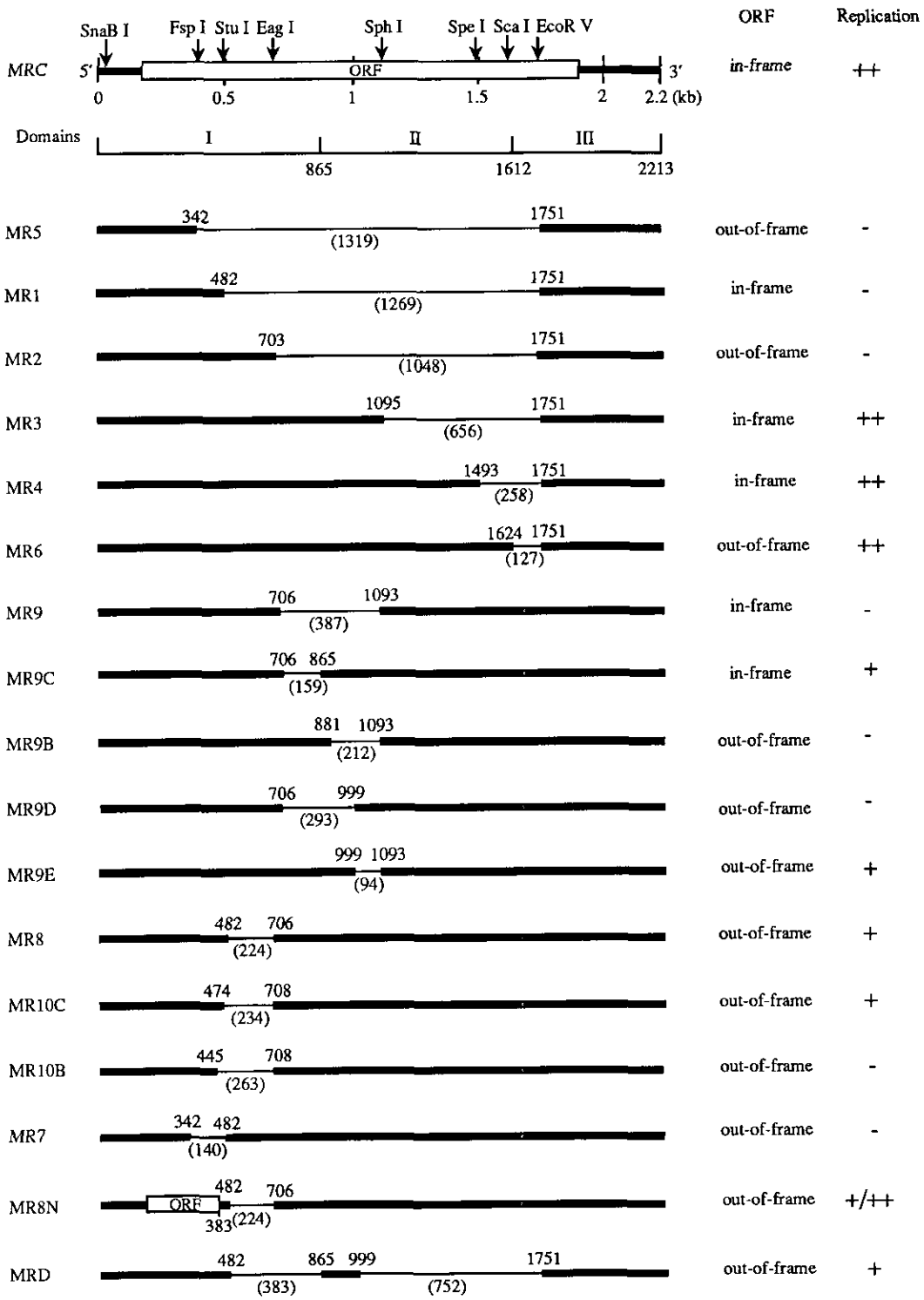

FIG. 2. Schematic diagram of the structure of MRC and MRC-derived internal deletion mutants. The DIssE-specific ORF is shown as a box. The *sequences deleted from MR5 through MRD are shown as thin lines. The number beneath each thin line indicates the number of nucleotides* deleted, and the exact location of each deleted region is shown as nucleotides numbered from the 5′ end of MRC. Restriction enzyme sites used in the construction of the deletion mutants are shown at the top of the diagram. The three domains of DIssE (domains I through III) are indicated beneath the diagram of MRC; the exact locations of the domain are numbered from the 5′ end of MRC. The number 383 shown beneath the MR8N-specific ORF represents the termination site of the MR8N-specific ORF. Deletions that interrupted the DIssE-specific ORF and that did not interrupt the DIssE-specific ORF are noted as out-of-frame and in-frame, respectively. DI RNAs which replicated at the same efficiency as MRC, those which replicated less efficiently than MRC, and those which did not replicate are indicated by ++, +, and −, respectively.

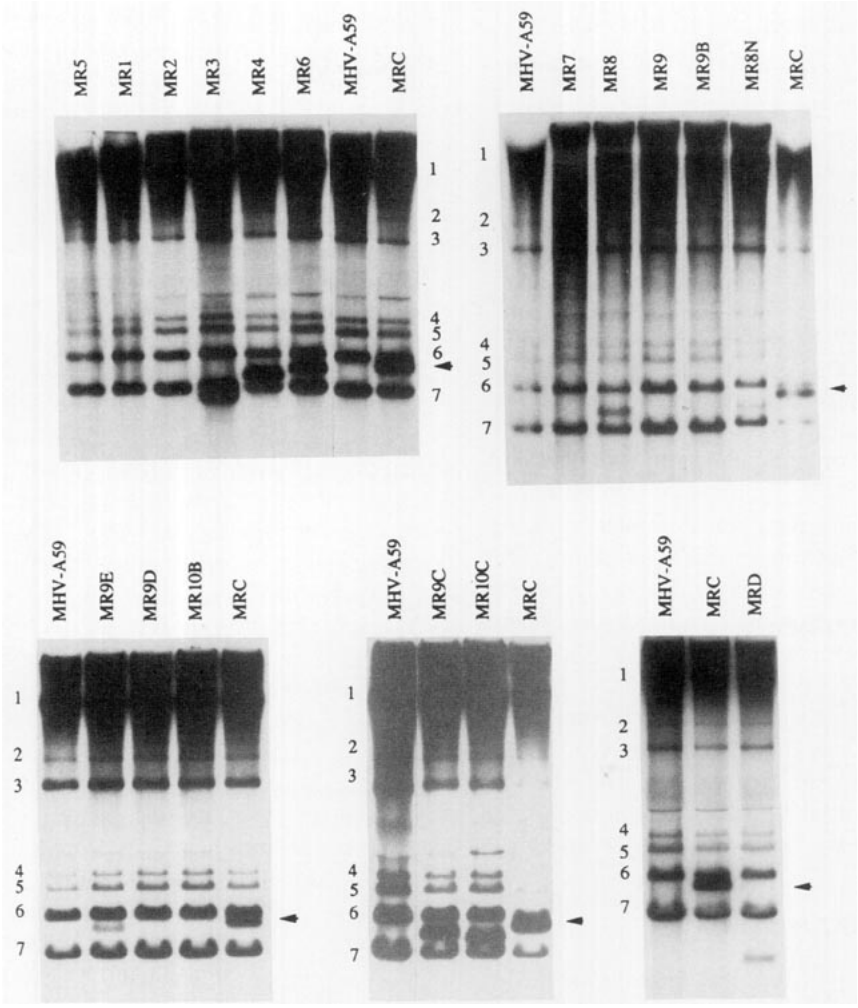

FIG. 3. Replication of MRC and MRC-derived internal deletion mutants in DI RNA-transfected, MHV-infected cells. Equal amounts of each *in vitro*-synthesized DI RNA were transfected into MHV-A59-infected DBT cells at 1 hr p.i. Intracellular RNA was labeled with ^{32}Pi for 2 hr in the presence of actinomycin D (2.5 μg/ml) at 5 hr p.i. RNAs were denatured with glyoxal and electrophoresed on 1% agarose gels. The MHV specific mRNA species are numbered 1 through 7. MRC DI RNA is shown by an arrowhead. The data in the five panels are the results from five independent experiments.

fection in the DI RNA-transfected cells (Jeong and Makino, 1992). The sequence of MR8N-specific negative-stranded RNA was examined as described in Materials and Methods. The 0.5-kb DI RNA-specific PCR product was generated by this PCR reaction, whereas the 2.8-kb-long negative-stranded MHV genomic RNA-specific PCR product was not detected (data not shown). The specificity of these reactions was demonstrated by repeating the reverse transcription and amplification procedure described above, using a sample containing a mixture of *in vitro*-synthesized MR8N DI RNA and intracellular RNA species from MHV-A59-infected cells. In this case, the synthesis of a DI RNA-specific PCR product was not observed (data not shown). Direct sequencing of the gel-purified DI RNA-specific PCR product demonstrated that the nucleotide deletion introduced in MR8N was maintained in the DI RNA-transfected cells (data not shown). This observation indicated that the absence of DI RNA replication in MR2, MR9B, MR9D, and MR10B was not due to the destruction of the large DIssE-specific ORF.

To examine whether the size of DI RNAs with the internal deletion was stable during virus passage, MRC, MR3, MR4, and MR9C, all of which contain the in-frame ORF were passaged once from DI RNA-transfected cells. Analysis of intracellular DI RNA species from the cells infected with those passaged virus samples demonstrated that all the DI RNAs maintained their expected sizes (data not shown).

The above data demonstrated that the MRC nucleotides from position 474 to 865 and 999 to 1751 were not needed for efficient DI RNA replication. To confirm these observations, a mutant was made that had three noncontiguous regions including positions 1 to 482, 865 to 999, and 1751 to the 3′ end of MRC. This mutant, MRD, replicated efficiently and produced RNA of the expected size in MRD RNA-transfected, MHV-infected cells (Figs. 2 and 3).

Replication effects of deletions from MHV-DI terminal sequences

To examine the effect on DI RNA replication of deletions at the 5′-region of DIssE-derived DI RNA, five deletion mutants, MR13–MR17, were constructed (Fig. 4A). An MRC-derived mutant, MRE, which contained an *Eco*RV site downstream of the genomic leader sequence was constructed and used as the reference clone for the 5′ end mutants (Fig. 4B). The MR13 leader sequence had 32 nucleotides deleted, and MR14 was deleted at the leader-body junction sequence (Fig 4B). Other DI RNAs contained a deletion downstream of the genomic leader sequence. Although MRE replicated efficiently, none of the deletion mutants did (data not shown).

The effect on DI RNA replication of a deletion at the 3′ region was similarly examined using mutants with sequences deleted downstream of the MRC *Eco*RV site (Fig. 4C). These 3′ end deletion mutants also failed to replicate in DI RNA-transfected cells (data not shown).

These analyses suggested that *cis*-acting replication signals necessary for MHV RNA replication were present at the 5′ end 474 nucleotides, the 3′ end 462 nucleotides and at an internal sequence located 3113 to 3247 nucleotides from the 5′ end of the genome.

DISCUSSION

By analysis of multiple, overlapping deletions, it was found that DIssE replication depended upon an internal sequence of flexible position and fixed sequences at its termini. The 5′-most 134 nucleotides of DIssE domain II, the 5′ end 474 nucleotides, and the 3′ end 462 nucleotides were required for efficient DIssE replication. These *cis*-acting DI RNA replication signals are present in all naturally occurring MHV DI RNAs examined to date (Makino *et al.*, 1985, 1988a, 1990; van der Most, 1991). It is now evident that one of the reasons why naturally occurring MHV DI RNAs have conserved these regions is because they are necessary for DI RNA replication.

DI RNAs with the 134-nucleotide long 5′-domain II region at position 865 to 999 (e.g., MRC and MR9E) and at position 482 to 616 (MRD) from the 5′ end, and at 1214 to 1348 nucleotides (e.g., MRC) and at 462 to 598 nucleotides (MRD) from the 3′ end replicated efficiently. The same region is mapped at 2.4 kb from the 3′ end of DIssF (Makino *et al.*, 1990), and in the MHV-A59-derived DI RNA, this region is mapped at 3.1 kb from the 5′ end and 2.3 kb from the 3′ end (van der Most *et al.*, 1991). Because this 134-nucleotide region was not fixed among the DI RNA genomes it seemed that a specific location was not important for its biological function.

Although the 134 nucleotides at the 5′ end of domain II were identified as essential for efficient DIssE replication, the minimum sequence required for biological function is not known. Also, the relative importance of the sequence and the RNA structure dictated by the sequence is not known. Sequence comparison of this region between MHV-JHM and MHV-A59 demonstrated that there are several nucleotide substitutions (Lee *et al.*, 1991; van der Most *et al.*, 1991) and the computer-generated secondary structure of this region differed between the two viruses (data not shown). By the computer analysis, the 134 nucleotides at the 5′ end of domain II was shown to have some sequence homology and complementarity with other regions of DIssE (data not shown), though the significance of this, if any, was not clear. It should be noted that for brome mosaic virus (BMV) the terminal sequences and a 150 nucleotide-long intercistronic region of RNA3 are necessary for efficient replication (French and Ahlquist, 1987). This intercistronic sequence is homologous to sequences found near the 5′ end of BMV RNA1 and RNA2 and lies in positions analogous to the three genomic RNAs of the related cucumber mosaic virus (French and Ahlquist, 1987). Consequently, these intercistronic sequences are considered to play a role in plus-strand RNA synthesis (French and Ahlquist, 1987). It was also shown that the BMV RNA3 intercistronic sequence is important for the regulation of asymmetric (+) and (−)-stranded BMV RNA replication (Marsh *et al.*, 1991). It is possible that the 134 nucleotides at the 5′ end of MHV DIssE domain II may interact with the virus-specific replication complex during replication, or perhaps the secondary or tertiary structure formed by this region interacting with either or both MHV RNA termini is important for MHV RNA replication. More study is needed to fully understand the role of the domain II-5′ region in efficient MHV DI RNA replication.

Introduction of deletions at the 5′ and 3′ ends of DI RNA revealed that the 5′-most 474 nucleotides and 3′-most 462 nucleotides are necessary for DI RNA replication. This result was expected since the viral RNA polymerase must interact specifically with these sequences or their complements in initiation of (−)- and (+)-strand RNA synthesis. Sequence analysis of coronavirus RNAs demonstrated that the GGAAGAGC sequence present near the 3′ end of MHV genome is conserved among coronaviruses and it was suggested that this sequence may be the recognition sequence of RNA polymerase (Lai, 1990). The data from this study agree with that speculation, because this conserved sequence was included within the 3′-*cis*-acting replication signals of MHV DI RNA. Although terminal *cis*-acting replication signals were identified, it is not known how much of the sequences at these regions is necessary for DI RNA replication. The data from this study

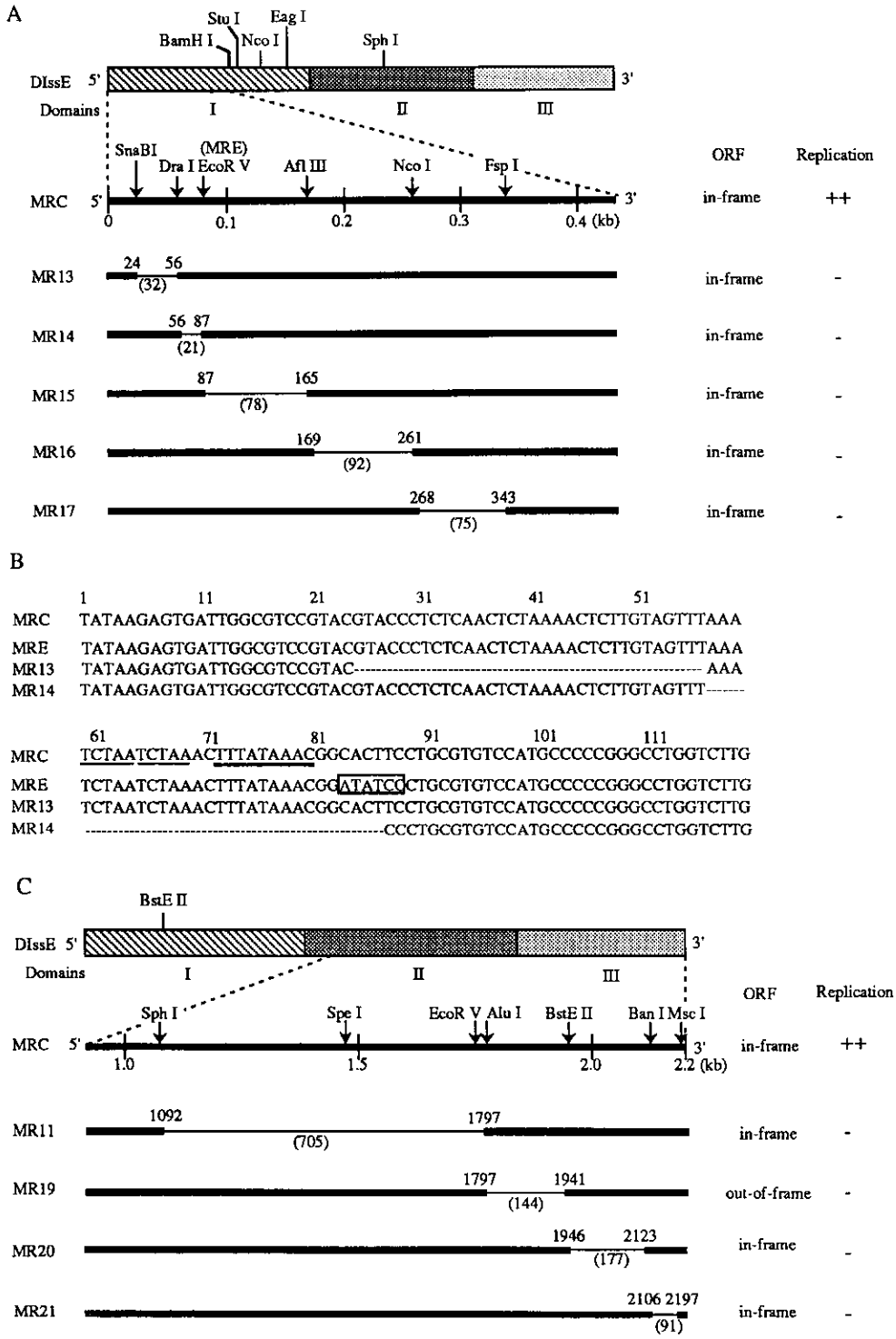

FIG. 4. Schematic diagram of MRC-derived mutants with 5'-region deletions (A, B) and with 3'-region deletions (C). (A) The diagrams depicted above are described in the legend for Fig. 2. The location of the MRE-specific *Eco*RV site is also shown. (B) Sequences of the 5'-regions of MRC, MRE, MR13 and MR14. The mutated nucleotides of MRE are boxed. The numbers shown above the sequences represent the nucleotide position from the 5' end of MHV-genomic RNA. The two UCUAA pentanucleotide repeats and the nine-nucleotide sequence (described in text) are shown by thin underlines and bold underlines, respectively. (C) Schematic diagram of MRC-derived mutants with 3'-region deletions. The diagrams depicted above are described in the legend for Fig. 2.

and preliminary data indicated that all of the terminal sequences are not necessary: MRE, with sequences mutated downstream of the genomic leader, replicated efficiently, and it was also found that several nucleotide substitutions and deletions at the termini did not significantly affect DI RNA replication efficiency (unpublished

data). It is not clear why the MHV RNA terminal *cis*-acting replication signals were longer than those of the alphavirus superfamily (French and Ahlquist, 1987; Levis *et al.*, 1986). It is possible that a number of important RNA sequences or/and structures are present within the termini and loss of one of these elements may significantly affect MHV RNA replication.

The UCUAA pentanucleotide repeat at the 3′-region of the genomic leader sequence is important for MHV transcription (Joo and Makino, 1992; Makino *et al.*, 1988b), though it is not certain whether the pentanucleotide repeat is necessary for MHV RNA replication. The nine-nucleotide UUAUAAAC sequence located downstream of the pentanucleotide repeat is not necessary for MHV RNA replication (Makino *et al.*, 1988b, 1989). In the present study it was found that MR14, with the pentanucleotide repeat and the nine nucleotides deleted, did not replicate in DI RNA-transfected, MHV-infected cells. These data suggested that the pentanucleotide repeat was requisite for efficient DI RNA replication.

It was proposed that coronavirus subgenomic mRNA species are amplified in mRNA replicons (Sethna *et al.*, 1989). This model and a number of published observations are not consistent. These include: the molar ratio of coronavirus subgenomic mRNA is essentially constant during MHV replication (Leibowitz *et al.*, 1981), replication of subgenomic DI RNA is not observed in the subgenomic DI RNA-transfected and MHV-infected cells (Makino *et al.*, 1991), and the molar ratio of a constant-sized subgenomic DI RNA to varying sizes of genomic DI RNAs is the same (Makino and Joo, 1993). As shown in the present study, MHV subgenomic mRNAs lack the internal 134 nucleotides and are missing all but the 70-nucleotide-long leader sequence of the 474 nucleotides at the 5′ end. Clearly MHV mRNA species do not contain all the necessary RNA replication signals. These pieces of data may indicate that coronavirus subgenomic mRNAs are not amplified by a replicon-type mechanism.

One characteristic feature of coronavirus DI RNAs is that all naturally occurring DI RNAs contain a large ORF which is a composite of different genomic regions (Makino *et al.*, 1988b, 1990; van der Most *et al.*, 1991). Although the synthesis of a DI RNA-specific protein is in fact detected in DI RNA-replicating cells (de Groot *et al.*, 1992; Kim *et al.*, 1993; Makino *et al.*, 1988a, 1990), the role of the DI-specific ORF in DI RNA replication is still not clear. A DIssE-derived mutant with an ORF reduced in size by nine-tenths replicates efficiently in DI RNA-transfected, MHV-infected cells (Kim *et al.*, 1993). The efficient replication of MR8N, MR6, MR8, MR9E, MR10C and MRD, all of which contained an interrupted ORF, supported that previous observation. Clearly, the large DI RNA-specific ORF is not necessary for DI RNA replication. Mutant MR10B, which was deleted at positions 445 to 708, did not replicate. This was probably not the result of an interrupted small ORF, but rather was due to the absence of some sequence between nucleotides 445 and 474, because MR8N, with a smaller ORF than that of MR10B, replicated efficiently. It is possible that MR7, MR16 and MR17 DI RNA failed to replicate because each of these DI RNAs contained an interrupted ORF upstream of nucleotide 383. The fact that the large ORF was not necessary for replication was similar to the situation in the alphavirus superfamily but quite different from that of poliovirus DI RNA, which requires an uninterrupted ORF for its replication (Hagino-Yamagishi and Nomoto, 1989; Kaplan and Racaniello, 1988).

ACKNOWLEDGMENTS

We thank Jennifer Fosmire for helpful comments on the manuscript. This work was supported by Public Health Service Grant AI29984 from the National Institutes of Health.

REFERENCES

AHLQUIST, P., STRAUSS, E. G., RICE, C. M., STRAUSS, J. H., HASELOFF, J., and ZIMMERN, D. (1985). Sindbis virus proteins nsP1 and nsP2 contain homology to nonstructural proteins from several RNA plant viruses. *J. Virol.* **53,** 536–542.

DE GROOT, R. J., VAN DER MOST, R. G., and SPAAN, W. J. M. (1992). The fitness of defective interfering murine coronavirus DI-a and its derivatives is decreased by nonsense and frame shift mutations. *J. Virol.* **66,** 5898–5905.

FOSMIRE, J. A., HWANG, K., and MAKINO, S. (1992). Identification and characterization of a coronavirus packaging signal. *J. Virol.* **66,** 3522–3530.

FRENCH, R., and AHLQUIST, P. (1987). Intercistronic as well as terminal sequences are required for efficient amplification of brome mosaic virus. *J. Virol.* **61,** 1457–1465.

GILMER, D., RICHARDS, K., JONARD, G., and GUILLEY, H. (1992). cis-Acting sequences near the 5′-termini of beet necrotic yellow vein virus RNAs 3 and 4. *Virology* **190,** 55–67.

HAGINO-YAMAGISHI, K., and NOMOTO, A. (1989). In vitro construction of poliovirus defective interfering particles. *J. Virol.* **63,** 5386–5392.

HIGUCHI, R. (1990). Recombinant PCR. *In* "PCR Protocols" (Michael A. Innis, David H. Gelfand, John J. Sninsky, and Thomas J. White, Eds.), pp. 177–183. Academic Press, San Diego.

HIRANO, N., FUJIWARA, K., HINO, S., and MATSUMOTO, M. (1974). Replication and plaque formation of mouse hepatitis virus (MHV-2) in mouse cell line DBT culture. *Arch. Gesamte. Virusforch.* **44,** 298–302.

JEONG, Y. S., and MAKINO, S. (1992). Mechanism of coronavirus transcription: duration of primary transcription initiation activity and effect of subgenomic RNA transcription on RNA replication. *J. Virol.* **66,** 3339–3346.

JOO, M., and MAKINO, S. (1992). Mutagenic analysis of the coronavirus intergenic consensus sequence. *J. Virol.* **66,** 6330–6337.

JUPIN, I., RICHARDS, K., JONARD, G., GUILLEY, H., and PLEIJ, C. W. A. (1990). Mapping sequences required for productive replication of beet necrotic yellow vein virus RNA 3. *Virology* **178,** 273–280.

KIM, Y.-N., LAI, M. M. C., and MAKINO, S. (1993). Generation and selection of coronavirus defective interfering RNA with large open reading frame by RNA recombination and possible editing. *Virology* **194,** 244–253.

KAPLAN, G., and RACANIELLO, V. R. (1988). Construction and charac-

terization of poliovirus subgenomic replicons. *J. Virol.* **62,** 1687–1696.

LAI, M. M. C. (1990). Coronavirus: Organization, replication and expression of genome. *Annu. Rev. Microbiol.* **44,** 303–333.

LAI, M. M. C., BARIC, R. S., BRAYTON, P. R., and STOHLMAN, S. A. (1984). Characterization of leader RNA sequences on the virion and mRNAs of mouse hepatitis virus, a cytoplasmic RNA virus. *Proc. Natl. Acad. Sci. USA* **81,** 3626–3630.

LAI, M. M. C., BRAYTON, P. R., ARMEN, R. C., PATTON, C. D., PUGH, C., and STOHLMAN, S. A. (1981). Mouse hepatitis virus A59: mRNA structure and genetic localization of the sequence divergence from hepatotropic strain MHV-3. *J. Virol.* **39,** 823–834.

LAI, M. M. C., PATTON, C. D., BARIC, R. S., and STOHLMAN, S. A. (1983). Presence of leader sequences in the mRNA of mouse hepatitis virus. *J. Virol.* **46,** 1027–1033.

LAI, M. M. C., and STOHLMAN, S. A. (1978). RNA of mouse hepatitis virus. *J. Virol.* **26,** 236–242.

LEE, H.-J., SHIEH, C.-K., GORBALENYA, A. E., EUGENE, E. V., LA MONICA, N., TULER, J., BAGDZHADZHYAN, A., and LAI, M. M. C. (1991). The complete sequence (22 kilobases) of murine coronavirus gene 1 encoding the putative proteases and RNA polymerase. *Virology* **180,** 567–582.

LEIBOWITZ, J. L., WILHELMSEN, K. C., and BOND, C. W. (1981). The virus-specific intracellular RNA species of two murine coronaviruses: MHV-A59 and MHV-JHM. *Virology* **114,** 39–51.

LEVIS, R., WEISS, B. W., TSIANG, M., HUANG, H., and SCHLESINGER, S. (1986). Deletion mapping of Sindbis virus DI RNAs derived from cDNAs defines the sequences essential for replication and packaging. *Cell* **44,** 137–145.

LUYTJES, W., KRYSTAL, M., ENAMI, M., PARVIN, J. D., and PALESE, P. (1989). Amplification, expression, and packaging of a foreign gene by influenza virus. *Cell* **59,** 1107–1113.

MAKINO, S., FUJIOKA, N., and FUJIWARA, K. (1985). Structure of the intracellular defective viral RNAs of defective interfering particles of mouse hepatitis virus. *J. Virol.* **54,** 329–336.

MAKINO, S., and JOO, M. (1993). Effect of intergenic consensus sequence flanking sequences on coronavirus transcription. *J. Virol.* **67,** 3304–3311.

MAKINO, S., JOO, M., and MAKINO, J. K. (1991). A system for study of coronavirus mRNA synthesis: a regulated, expressed subgenomic defective interfering RNA results from intergenic site insertion. *J. Virol.* **65,** 6031–6041.

MAKINO, S., and LAI, M. M. C. (1989). High-frequency leader sequence switching during coronavirus defective interfering RNA replication *J. Virol.* **63,** 5285–5292.

MAKINO, S., SHIEH, S.-K., SOE, L. H., BAKER, S., and LAI, M. M. C. (1988a). Primary structure and translation of a defective interfering RNA of murine coronavirus. *Virology* **166,** 550–560.

MAKINO, S., SOE, L. H., SHIEH, C.-K., and LAI, M. M. C. (1988b). Discontinuous transcription generates heterogeneity at the leader fusion sites of coronavirus mRNAs. *J. Virol.* **62,** 3870–3873.

MAKINO, S., TAGUCHI, F., and FUJIWARA, K. (1984a). Defective interfering particles of mouse hepatitis virus. *Virology* **133,** 9–17.

MAKINO, S., TAGUCHI, F., HIRANO, N., and FUJIWARA, K. (1984b). Analysis of genomic and intracellular viral RNAs of small plaque mutants of mouse hepatitis virus, JHM strain. *Virology* **139,** 138–151.

MAKINO, S., YOKOMORI, K., and LAI, M. M. C. (1990). Analysis of efficiently packaged defective interfering RNAs of murine coronavirus: Localization of a possible RNA-packaging signal. *J. Virol.* **64,** 6045–6053.

MARSH, L. E., HUNTLEY, C. H., POGUE, G. P., CONNELL, J. P., and HALL, T. C. (1991). Regulation of (+):(−) strand asymmetry in replication of brome mosaic virus RNA. *Virology* **182,** 76–83.

MCMASTER, G. K., and CARMICHAEL, G. G. (1977). Analysis of single- and double-stranded nucleic acids on polyacrylamide and agarose gels by using glyoxal and acridine orange. *Proc. Natl. Acad. Sci. USA* **74,** 4835–4838.

PACHA, R. F., ALLISON, R. F., and AHLQUIST, P. (1990). cis-Acting sequences required for in vivo amplification of genomic RNA3 are organized differently in related bromoviruses. *Virology* **174,** 436–443.

PACHUK, C. J., BREDENBEEK, P. J., ZOLTICK, P. W., SPAAN, W. J. M., and WEISS, S. R. (1989). Molecular cloning of the gene encoding the putative polymerase of mouse hepatitis virus, strain A59. *Virology* **171,** 141–148.

SAWICKI, S. G., and SAWICKI, D. L. (1990). Coronavirus transcription: Subgenomic mouse hepatitis virus replicative intermediates function in RNA synthesis. *J. Virol.* **64,** 1050–1056.

SETHNA, P. B., HOFMANN, M. A., and BRIAN, D. A. (1989). Coronavirus subgenomic minus-strand RNAs and the potentional for mRNA replicons. *Proc. Natl. Acad. Sci. USA* **86,** 5626–5630.

SPAAN, W., DELIUS, H., SKINNER, M., ARMSTRONG, J., ROTTIER, P., SMEEKENS, S., VAN DER ZEIJST, and SIDDELL, S. G. (1983). Coronavirus mRNA synthesis involves fusion of non-contiguous sequences. *EMBO J.* **2,** 1939–1944.

VAN DER MOST, R. G., BREDENBEEK, P. J., and SPAAN, W. J. M. (1991). A domain at the 3′ end of the polymerase gene is essential for encapsidation of coronavirus defective interfering RNAs. *J. Virol.* **65,** 3219–3226.

VAN DER MOST, R. G., HEIJNEN, L., SPAAN, W. J. M., and DE GROOT, R. J. (1992). Homologous RNA recombination allows efficient introduction of site-specific mutations into the genome of coronavirus MHV-A59 via synthetic co-replicating RNAs. *Nucleic Acids Res.* **20,** 3375–3381.

WINSHIP, P. R. (1989). An improved method for directly sequencing PCR material using demethyl sulfoxide. *Nucleic Acids Res.* **17,** 1266.